Part VIII
Dark Matter and Ω_0

https://doi.org/10.1017/S0074180900216355 Published online by Cambridge University Press

New Cosmological Data and the Values of the Fundamental Parameters
IAU Symposium, Vol. 201, 2005
Anthony Lasenby and Althea Wilkinson, eds.

Ω_0 Concordance

Masataka Fukugita

University of Tokyo, Institute for Cosmic Ray Research, Kashiwa, 2778582, Japan

Institute for Advanced Study, Princeton, NJ 08540, USA

Abstract. The determinations of the mass density parameter Ω_0 are examined with a particular emphasis given to the new cosmic microwave background (CMB) experiments. It is shown that the Ω_0 and the Hubble constant H_0 from CMB are quite consistent with those from other observations with the aid of the hierarchical structure formation models based on cold dark matter dominance with the cosmological constant that makes the universe flat. The concordance value of Ω_0 is 0.25–0.45.

1. Introduction

Among the three cosmological parameters that govern the evolution of the Friedmann universe, the density parameter $\Omega_0 = \rho/\rho_{\rm crit}$ dominantly controls the gravitational formation of cosmic structure. There are a number of methods to determine Ω_0 from observations, some of them without referring to specific structure formation models and others based on the hierarchical clustering model assuming the cold dark matter (CDM) dominance. The extraction of Ω_0 in the latter is necessarily model-dependent, but this very fact makes the determination of Ω_0 particularly useful in testing the validity of the structure formation model. Whether Ω_0's from various observations with and without models converge to a unique value is an important cosmological test; an accurate test would even 'prove' the existence of dark matter even prior to its direct observations.

Table 1 gives a summary of Ω_0 from various observations. This list points to low value, yet there are variations from $\Omega_0 \simeq 0.1-0.2$ to $0.4-0.5$, more than by a factor of 2. In this talk we re-examine some of these determinations, with a particular emphasis given to the information we can extract from the recent cosmic microwave background (CMB) experiments of Boomerang (de Bernardis 2000) and MAXIMA (Hanany et al. 2000). The items which will be examined in this article are denoted by asterisks in the table.

2. Constraints from CMB anisotropies

2.1. Parametric approach

The fluctuations imprinted on CMB are the result of integration over all information concerning the evolution of the universe and the density perturbations. Therefore, accurate measurements of the CMB harmonics are eligible to pro-

Table 1. Summary of Ω_0 (as of 1999). Asterisks indicate items examined in this article

method	Ω_0	
`model independent`:		
H_0 vs t_0	$< 0.86 - 0.9$	
luminosity density +M/L	0.1–0.3	*
cluster baryon fraction	0.05–0.5	*
SNeIa Hubble diagram	0.13–0.47 (flat)	
	≈ 0 (open)	
small-scale velocity field (summary)	0.2 ± 0.15	
(pairwise velocity)	0.15 ± 0.1	
(Local Group kinematics)	0.15 ± 0.15	
(Virgocentric flow)	0.2 ± 0.2	*
large-scale velocity field	0.2–1	
gravitational lensing	> 0.2 (flat)	
	no constraint (open)	
`model dependent`:		
cluster evolution (low Ω sol'n)	$0.2^{+0.3}_{-0.1}$	
(high Ω sol'n)	~ 1	
COBE-cluster matching ($n = 1$)	0.35–0.45 (if $\lambda = 0$)	
	0.20–0.40 (if $\lambda \neq 0$)	*
shape parameter Γ	0.15–0.30	
CBR acoustic peak	$1 - \lambda_0$ (flat)	*
	> 0.5 (open)	
summary	0.15–0.45 (if open)	
	0.2–0.4 (if flat)	

vide us with a robust tool to study cosmological parameters. With the recent experiments of Boomerang and MAXIMA this expectation has come closer to being realised. A number of analyses have followed the data releases, reported optimal cosmological parameters, mostly using maximum likelihood analyses in multidimensional parameter space with a variety of prior assumptions (Lange et al. 2000; Tegmark & Zaldarriaga 2000; Balbi et al. 2000; Jaffe et al. 2000; Bridle et al. 2000). While these analyses are complete and valuable, the high dimension of parameter space makes it difficult to understand the physics that characterises the derivation of specific constraints and the interplay of the prior assumptions and the results. Therefore, we have taken a different approach to this problem (Hu et al. 2000), the result of which I describe in this section. The starting point is that the detailed behaviour of the harmonics is not very important with the present accuracy, but they are characterised by a relatively small number of parameters. We then study how these parameters depend on the cosmological parameters to derive constraints.

We choose four parameters: the position of the first peak ℓ_1, the height of the first peak relative to the large scale power taken at $\ell = 10$, $H_1 =$

https://doi.org/10.1017/S0074180900216355 Published online by Cambridge University Press

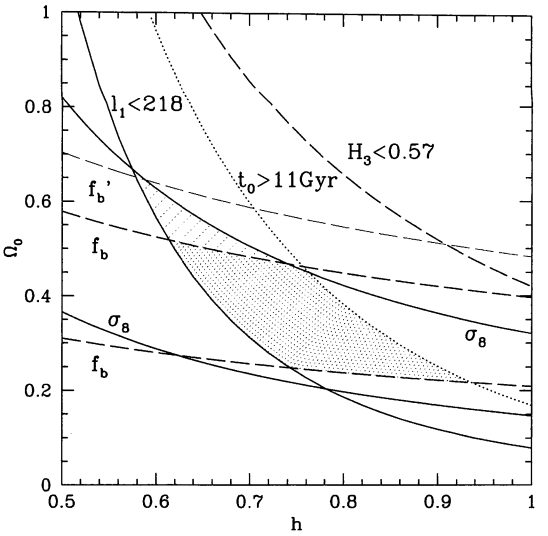

Figure 1. Constraints derived from the position of the first peak of CMB, $\ell_1 < 218$ and from H_3. Allowed region is indicated by hatching. The isochronal contour corresponding to 13.2 Gyr is also plotted.

$(\Delta T_{\ell_1}/\Delta T_{10})^2$, the height of the second peak relative to the first $H_2 = (\Delta T_{\ell_2}/\Delta T_{\ell_1})^2$, and the height of the third relative to the second $H_3 = (\Delta T_{\ell_3}/\Delta T_{\ell_1})^2$, where $(\Delta T_\ell)^2 = \ell(\ell+1)C_\ell/2\pi$ with C_ℓ the power spectrum of the multipole moments of the temperature field. We define the positions of the second and third peaks as those expected from the first, since the higher harmonics peaks are not conspicuous and the positions are empirically ambiguous. We combine the Boomerang and MAXIMA data and use model CMB multipoles with a wide variety of parameters as templets to determine the four parameters. The normalisations of the observed C_ℓ are shifted within the claimed uncertainties. We obtain: $\ell_1 = 206 \pm 6$, $H_1 = 7.6 \pm 1.4$, $H_2 = 0.38 \pm 0.04$ and $H_3 = 0.43 \pm 0.07$. We adopt one standard deviation when we quote errors, but consider all constraints at two standard deviations.

We assume a flat ($\Omega_0 + \lambda_0 = 1$) geometry throughout our analysis, since open geometry is inconsistent with the observations.

2.2. Constraints from the CMB data alone

The position of the first peak is determined by the ratio of the comoving angular diameter distance to the last scattering epoch and the sound horizon at that epoch (Hu & Sugiyama 1995). This is the parameter that depends solely on geometry and acoustic dynamics. The dependence on spectral index n (tilt) is at most 3%. The observed position of the first peak gives a solid constraint in the $h - \Omega_0$ plane, where h is the Hubble constant in units of 100 km s^{-1}Mpc^{-1}. Particularly interesting to us is a limit on h and Ω_0 from below, corresponding

https://doi.org/10.1017/S0074180900216355 Published online by Cambridge University Press

to $\ell_1 < 218$. The constraint depends on Ω_b, and the most conservative limit is obtained at the lowest baryon abundance. Figure 1 shows the limit we derived from $\ell_1 < 218$ at 95% confidence level, as evaluated at $\Omega_b h^2 = 0.019$, which is derived from the CMB data, as we discuss later. The limit derived from $\ell_1 > 194$ is weak, but also it further weakens with a higher baryon abundance, while the baryon abundance indicated by the CMB data alone is practically unbounded towards its high side; hence we do not obtain a meaningful limit on the $h - \Omega_0$ plane from above. The constraint is summarised as

$$\Omega_0 h^{3.85} > 0.079 \ . \tag{1}$$

This is nearly parallel to an isochronal contour of $t < 13.2$ Gyr, although there is no logical reason that the two agree. As a conservative limit we obtain $t_0 < 14$Gyr.

The ratio of the heights of the second peak to the first primarily depends on the tilt parameter and the baryon abundance (Hu 2000). This combination is insensitive to reionisation, the presence of tensor modes or any effects that are confined to the low multipoles. The remaining sensitivity is to $\Omega_0 h^2$, which is modest in a flat universe due to some cancellations. The limit we obtained is given approximately by

$$\Omega_b h^2 > 0.0235 + 0.028 \left(\frac{\Omega_0 h^2}{0.15} \right)^{-0.58} (n-1) \ . \tag{2}$$

The dependence of H_1 to the cosmological parameters is more complicated, but fortunately, most complications tend to decrease H_1 by adding large scale anisotropies. Therefore, the lower limit on n from the lower limit of H_1 in the absence of reionisation and tensor mode gives a conservative constraint. We then search for the minimum n that gives $H_1 > 4.8$ along the parameter space that maximises H_2. This gives a conservative limit on n as in

$$n > 0.85 \ . \tag{3}$$

With the aid of (2), this translates to a lower limit on Ω_b

$$\Omega_b h^2 > 0.019 \ . \tag{4}$$

The ratio H_3 depends more strongly on $\Omega_0 h^2$ and n; the baryon affects the heights of the third and first peaks in a similar way. The observed small H_3 leads to an upper limit on $\Omega_0 h^2$ as a function of n. When supplemented with the lower limit on n, we get

$$\Omega_0 h^2 < 0.42 \ , \tag{5}$$

as the most conservative limit. This is also plotted in Figure 1 above.

We examined our constraints with a general likelihood analysis of Tegmark & Zaldarriaga (2000) and confirmed that they do not differ from the likelihood results by more than a few percent. When the two results do not agree, the allowed region from the likelihood analysis is limited by imposed prior conditions.

https://doi.org/10.1017/S0074180900216355 Published online by Cambridge University Press

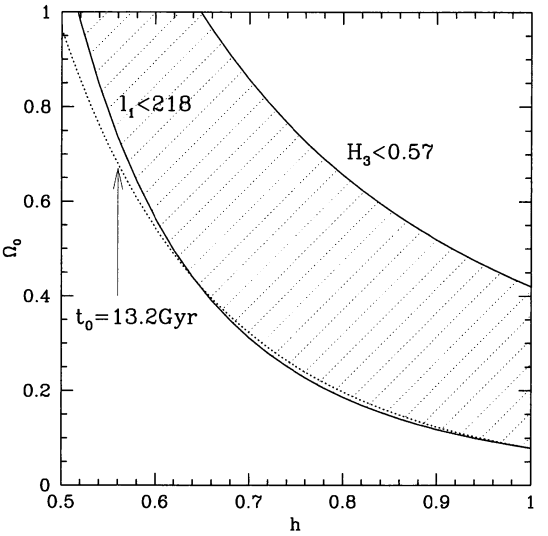

Figure 2. Summary of constraints from the CMB analysis with the aid of three external constraints, primordial nucleosynthesis, the rich cluster abundance and the cluster baryon fraction. The allowed region is shown by dark shading, while the light shaded region is allowed when the constraint from nucleosynthesis is somewhat relaxed as described in section 2.3.

2.3. Constraints using external information

The constraints on n and Ω_b can be mapped into those on the $h - \Omega_0$ plane if appropriate external constraints are employed. We choose three constraints (i) the baryon abundance from primordial nucleosynthesis, (ii) the rich cluster abundance at $z \approx 0$ and (iii) the cluster baryon fraction.

Baryon abundance from primordial nucleosynthesis has been discussed over many years (see Olive et al. 1999; Tytler 2000 for recent reviews). Olive et al. give two solutions, a high baryon density option of $0.015 \leq \Omega_b h^2 < 0.023$, and a low baryon density option $0.004 \leq \Omega_b h^2 < 0.010$ at the 95% confidence. A low baryon option is motivated by the traditional low value of helium abundance ($Y_p = 0.234 \pm 0.003$) and it points to a high deuterium abundance. This is consistent with two Lyman limit systems (Tytler et al. 1999 and references therein). This low baryon solution is excluded by limit (4) from the CMB.

On the other hand, the high baryon option is driven by the recently more favoured low deuterium abundance, the literal value being D/H=$(3.4 \pm 0.25) \times 10^{-5}$. Tytler (2000) claims an even smaller error for the baryon abundance, $\Omega_b h^2 = 0.019 \pm 0.0012$. This high baryon option agrees with $Y_p = 0.244 \pm 0.002$ derived by Izotov & Thuan (1998), which is inconsistent with the traditional estimate. The origin of this discrepancy is of systematic nature, mainly arising from the use of different helium recombination rates and different corrections for the collisional excitation. We adopt $\Omega_b h^2 < 0.023$ of Olive et al. as the upper

https://doi.org/10.1017/S0074180900216355 Published online by Cambridge University Press

limit, but also we allow for the possibility that the actual baryon abundance would be somewhat higher, $\Omega_b h^2 < 0.028$, which corresponds to D/H=2×10^{-5} (the interstellar D/H value with modest destruction of deuterium by stars) and $Y_p = 0.250 - 0.252$ (3-4 sigma from the Izotov-Thuan value, taking their error estimate literally).

With $\Omega_b h^2 < 0.023$, when combined with (3), we obtain

$$0.85 < n < 0.98 \ , \tag{6}$$

and with $\Omega_b h^2 < 0.028$,

$$0.85 < n < 1.16 \ . \tag{7}$$

We can fit the low second peak only at two sigma, and a red tilt is needed if we impose the consistency with the conventional baryon abundance.

This limit on the tilt parameter is combined with the matching condition of the cluster abundance versus CMB fluctuations to give a constraint on the $h - \Omega_0$ plane. We adopt the empirical fit of Eke et al. (1996) for the cluster abundance in the flat universe, $\sigma_8 = (0.52 \pm 0.08)\Omega_0^{-0.52+0.13\Omega_0}$, and take the two sigma range as allowed. The empirical value of σ_8 is well converged within 1 sigma among different authors. This is because the cluster abundance depends strongly on σ_8 due to its appearance in the exponential of a Gaussian function in the Press-Schechter formalism. With the amplitude at COBE scales with a 14% normalisation uncertainty (95% confidence) (Bennett et al. 1996; Bunn & White 1997) we obtain a constraint, which is expressed roughly

$$0.27 < \Omega_0^{0.76} h n < 0.35 \ , \tag{8}$$

assuming no tensor contributions to COBE and evaluated at $\Omega_b h^2 = 0.028$. The upper limit comes from overshooting σ_8 and depends on the lower limit on n, which only tightens with the inclusion of tensors and lowering the baryon density. The lower limit comes from undershooting σ_8 which is exacerbated with the inclusion of tensors, and maximised at the highest acceptable baryon density, but this limit is already in the region disfavoured by the baryon fraction argument.

The significance of our new constraint over similar ones in the previous work is that we have relaxed the assumption on the tilt parameter (which was usually assumed to be flat) and the allowance for a possible higher baryon density, as the CMB itself suggests. Therefore, what we get here is a quite conservative constraint without *ad hoc* assumptions

The third external constraint we consider is the baryon fraction in rich clusters form X ray observations. The observed baryon fraction shows a slight increase outwards, and the true baryon faction inferred for the entire cluster depends on the extrapolation. The estimate ranges from $(0.052 \pm 0.0025)h^{-3/2}$ (White & Fabian 1995) to $(0.076 \pm 0.008)h^{-3/2}$ (Arnaud & Evrard 1999). We take the 2 sigma limit to correspond to the two extreme edges. Adding baryons frozen into stars, and require the cluster baryons to agree with the global value, we obtain

$$\frac{0.019}{0.076h^{1/2} + 0.015h} < \Omega_0 < \frac{0.023}{0.052h^{1/2} + 0.006h} \ , \tag{9}$$

https://doi.org/10.1017/S0074180900216355 Published online by Cambridge University Press

for $0.019 < \Omega_b h^2 < 0.023$ or

$$\frac{0.019}{0.076h^{1/2} + 0.015h} < \Omega_0 < \frac{0.028}{0.052h^{1/2} + 0.006h}\ , \tag{10}$$

for $0.019 < \Omega_b h^2 < 0.028$.

Figure 2 shows our summary. The light shading is the allowed region with $\Omega_b h^2 < 0.028$ and the dark one is with the conventional baryon abundance limit $\Omega_b h^2 < 0.023$. We have drawn one more constraint on cosmic age $t_0 > 11$ Gyr from stellar evolution of globular clusters. While this is not based on a statistical analysis, no authors have ever claimed cosmic age shorter than this value (Gratton et al. 1997; Reid 1997; Chaboyer et al. 1998).

The shaded region does not mean that all models in this region are consistent with the CMB data. A viable model with a given (h, Ω_0) is constructed with an appropriate choice of n and Ω_b.

3. Ω_0 from other observations

There are a number of determinations of the mass density parameter, as we have listed in Table 1 earlier in this article. We include the Hubble constant in our list here, since we have always discussed the constraint in the $h - \Omega_0$ plane in section 2. We limit our considerations to the flat (non-zero Λ) universe, since the open universe grossly conflicts with the CMB observations.

3.1. Hubble constant

Supernova Hubble diagrams and surface brightness fluctuations (SBF) are among the most accurate secondary distance indicators. The Hubble constant from SNIa Hubble diagram is converged to 64 ± 3 km s^{-1}Mpc^{-1} using the calibration with the Saha-Sandage Cepheid distance (Saha et al. 1999) to local SN host galaxies. The HST-KP group carried out a reanalysis of the Saha-Sandage Cepheid distance, and found that all their distances are longer by 5-15% than are obtained with the HST-KP Cepheid analysis procedure, while the reasons vary from one to another (Gibson et al 2000; Freedman personal communication). With this calibration H_0 from SNeIa becomes 69 ± 3 km s^{-1}Mpc^{-1}. The most extensive analysis of SBF with 300 galaxies results in 77 ± 8 km s^{-1}Mpc^{-1} or with the aid of the peculiar velocity flow information from the galaxy distribution 74 ± 4 km s^{-1}Mpc^{-1} (Blakeslee et al. 1999). Considering both SNIa and SBF, we take 71 ± 7 km s^{-1}Mpc^{-1} as the two sigma overlapping range.

The value of H_0 here assumes the LMC distance of 50 kpc. Recent work on the local distance ladder shows that the distance to LMC is more uncertain than was thought. It varies from 43 to 53 kpc. This discrepancy is clearly of systematic nature, and hence we leave this uncertainty as an error to the Hubble constant. We conclude $H_0 = (71 \pm 4) \times (1.15 - 0.95)$. This summary is compared with the most recent HST-KP result $73 \pm 2 \pm 6$ km s^{-1}Mpc^{-1} (Freedman 2000). For more discussion, see Fukugita (2000).

3.2. Ω_0 from $\langle M/L \rangle$ and the luminosity density

The mass density is estimated by multiplying the luminosity density, $\mathcal{L}_B = (2.2 \pm 0.3) \times 10^8 h L_\odot$ Mpc^{-3}, with the average mass to light ratio $\langle M/L_B \rangle$ of

https://doi.org/10.1017/S0074180900216355 Published online by Cambridge University Press

galaxies (Peebles 1971). If the dark matter distribution is isothermal, the value of M/L_B inside the virial radius ($r = 0.13$ Mpc $\Omega_0^{-0.15}[M/10^{12}M_\odot]^{1/2}_{<100\mathrm{kpc}}$ in a spherical collapse model) is $(150-350)h$ for L^* galaxies. This is a little smaller than the value for groups and clusters, $(250-500)h$, from dynamics (Bahcall, Lubin & Dorman 1995) and from lensing (e.g. Kaiser et al. 1998). Multiplying the two values we get $\Omega_0 = 0.20 \pm 0.08$.

This conventional estimate assumes that light is a good tracer of mass and M/L is constant over a wide range of luminosity; it does not include the unclustered component, which is expected in the hierarchical clustering scenario and the increase of the mass to light ratio for small galaxies. To account for small galaxies and unclustered component, we consider galaxies with $L > (1/10)L^*$ and assume the average value of mass to light ratio for these galaxies. According to the CDM model ($\Omega_0 = 0.3$, $h = 0.7$, $\sigma_8 = 0.9$) the fraction of mass in galaxies with $M > (1/10)M^*$ is 60% of the total mass. This means that we must multiply the Ω_0 estimated from luminous galaxies by a factor of 1.3-1.5, giving $\Omega_0 = 0.16 - 0.43$.

3.3. Type Ia supernova Hubble diagram

Taking the 2 sigma error contour given in the paper (Riess et al. 1998; Perlmutter et al. 1999) the allowed range of the mass density for the flat universe is $\Omega_0 = 0.13 - 0.47$

3.4. Peculiar velocities and density enhancement

It has been known that Virgocentric flow observed at around the Local Group corresponds to a small mass density, $\Omega_0 \simeq 0.2$ (Peebles 1999). We studied, using a cosmological simulation of the CDM universe with $\Omega_0 \simeq 0.4$ as input (Cen & Ostriker 1999), whether such estimates give the correct value for the global mass density (Nagamine et al. in preparation). We examined infall peculiar velocities of test particles (galaxies) in the vicinity of large groups and clusters with a density enhancement $\delta > 5 - 10$, and calculated Ω_0 applying a spherical model just as we do for the Virgocentric infall for the Local Group. We found that the Ω_0 derived in this way varies wildly from 0 to 1, while the mean is located about the correct value. It was also found that if luminous components are used to calculate the overdensity of clusters, the mean becomes smaller than the correct value by a factor of 2. This indicates that the Virgocentric infall of the Local Group is not a robust indicator for Ω_0. To obtain the correct global mass density, we need a large sample of test particles with a proper control over the biasing of the luminous matter.

Ω_0 from the large scale flow (including the redshift distortion) is controversial. It varies from $\Omega_0 = 0.2$ to unity; see Dekel (1999).

3.5. Gravitational lensing frequency

The most important uncertainty in the current analysis is not in the size of the lensing sample, but in the calculation of the lensing power from galaxy statistics. Continuous efforts for nearly a decade have brought substantial improvement in reducing uncertainties in the normalisation factor. Nevertheless, the luminosity density of early type galaxies which dominantly affects the lensing power is

still uncertain by about a factor of two. The reason that Kochanek and his collaborators (Kochanek 1997; Falco et al. 1998) obtained a very stringent limit on λ_0 is their use of a large E/S0 luminosity density derived from the CfA luminosity function (Marzke et al. 1994) and a small error assumed in calculating the likelihood function. Some new lensing statistics analyses presented at this Conference adopt the lensing power estimated by Kochanek; so they give the limits on λ_0 that differ little from Kochanek's result. It seems clear that λ_0 in excess of 0.8 is excluded because of a sharp increase of the lensing frequency towards a higher λ_0, but the value below 0.8 is unlikely to be ruled out, since a shift of the luminosity density baseline by 50% easily modifies such a limit There are some works which claimed positive λ_0 as the most likely value, but for the same reason such results are also liable to be elusive. We take a conservative limit $\lambda_0 < 0.8$ which is not too sensitive to this concern.

3.6. Power spectrum of galaxies

There are no changes from the analyses of Efstathiou et al. (1990) and Peacock and Dodds (1994). We take $\Gamma + (n-1)/2 = 0.15 - 0.30$ (Bond & Jaffe 1999), where the spectral shape parameter is $\Gamma \approx \Omega_0 h \exp[-\Omega_b(1+\Omega_0^{-1})]$ (Sugiyama 1995). Although the expressions depend on n and Ω_b, they give only small corrections; hence we take this constraint as being independent from CMB.

3.7. Cluster abundance evolution

The matter density can be inferred from evolution of the rich cluster abundance (Oukbir & Blanchard 1992; Bahcall & Fan 1998). The current results, however, are controversial, depending sensitively on the estimate of the cluster masses at high redshift. We do not use this argument as a constraint.

4. Conclusion

Figure 3 presents all constraints discussed here in the $h - \Omega_0$ plane. The constraints derived from new CMB experiments overlap with those from other observations well in the flat universe. Another significance is that the (Ω_0, h) parameters derived via structure formation models agree with each other, but also with those from model-independent analyses, corroborating our understanding of cosmology and structure formation based on the CDM dominance. The convergent values are $\Omega_0 = 0.25 - 0.45$ ($\lambda_0 = 1 - \Omega_0$), and $h = 0.65 - 0.85$.

On the other hand, there is one aspect which would falsify the current understanding with increasing accuracies of CMB observations. If the errors would be reduced while the central values of the data remain as they are, the baryon abundance from the CMB will not be reconciled with primordial nucleosynthesis. This would also raise the problem as to where are these baryons today. The high baryon option taken in this article ($\Omega_b h^2 \simeq 0.02$) requires 3/4 of the baryons being hidden in the vicinity of galaxies and groups of galaxies as warm gas, yet marginally consistent with various observations (Fukugita, Hogan & Peebles 1998).

Most determinations of Ω_0 still allows the range that spreads by a factor of two. It seems that the work imminent to be done is to investigate systematic

https://doi.org/10.1017/S0074180900216355 Published online by Cambridge University Press

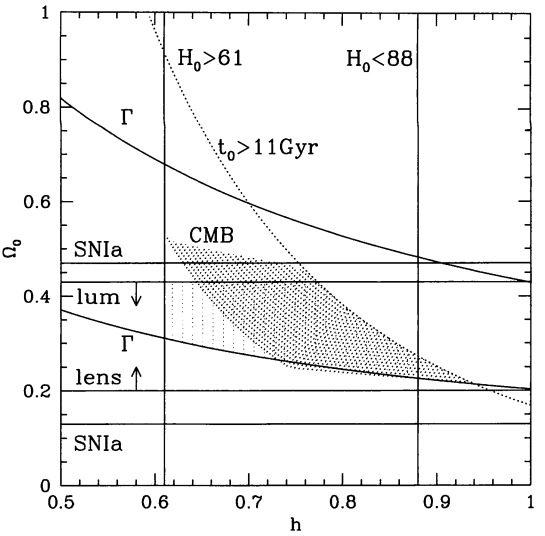

Figure 3. Consistency of all constraints discussed in this article. The region allowed by CMB with the aid of the three external constraints (Figure 2) are shown by dark shading. The region allowed by all other constraints is shown by light (vertical) hatching.

errors of each method and to reduce the error by a factor of two in time for the advancement that will be brought by the on-going CMB experiments, DASI, CSI and MAP.

I am grateful to my collaborators, R. Cen, W. Hu, K. Nagamine, J. Ostriker, J. Peebles, M. Tegmark and M. Zaldarriaga. This work is supported in Tokyo by Grant in Aid of the Ministry of Education of Japan, and in Princeton by Raymond and Beverly Sackler Fellowship.

References

Arnaud, M. & Evrard, A. E. 1999, MNRAS, 305, 631
Bahcall, N. A. & Fan, X. 1998, ApJ, 504,1
Bahcall, N. A., Lubin, L. M. & Dorman, V. 1995, ApJ, 447, L81
Balbi, A. et al. 2000, astro-ph/0005124
Bennett, C. L. et al. 1996, ApJ, 464, L1
de Bernardis, P. et al. 2000, Nature, 404, 955
Blakeslee, J. P. et al. 1999, ApJ, 527, L73
Bond, J. R. & Jaffe, A. H. 1999, Phil. Trans. Roy. Soc. London, 357, 57
Bridle, S. L. et al. 2000, astro-ph/0006170
Bunn, E. F. & White, M. 1997, M. ApJ, 480, 6
Cen, R. & Ostriker, J. P. 1999, ApJ, 514, 1

Chaboyer, B., Demarque, P. Kernan, P. J. & Krauss, L. M. 1998, ApJ, 494, 96
Dekel, A. 1999, astro-ph/9911501
Efstathiou, G., Sutherland, W. J. & Maddox, S. J. 1990, Nature, 348, 705
Eke, V. R., Cole, S., & Frenk, C. S. 1996, MNRAS, 282, 263
Falco, E. E., Kochanek, C. S. & Munoz, J. A. 1998, ApJ, 494, 47
Freedman 2000, these proceedings
Fukugita, M. 2000, in Structure Formation in the Universe, Proc. NATO ASI, Cambridge (1999) (to be published) [astro-ph/0005069]
Fukugita, M., Hogan, C. J. & Peebles, P. J. E. 1993, Nature, 366, 309
Gibson, B. K. et al. 2000, ApJ, 529, 723
Gratton, R. G. et al. 1997, ApJ, 491, 749
Hanany, S. et al. 2000, astro-ph/0005123
Hu, W. 2000, Nature, 404, 939
Hu, W. Fukugita, M. Zaldarriaga, M & Tegmark, M. 2000, astro-ph/0006436
Hu, W. & Sugiyama, N. 1995, Phys. Rev., D51, 2599
Izotov, Y. I & Thuan, T. X. 1998, ApJ, 500, 188
Jaffe, A. et al. 2000, astro-ph/0007333
Kaiser, N. et al. 1998, astro-ph/9809268
Kochanek, C. S. 1997, ApJ, 491, 13
Lange, A. E. et al. 2000, astro-ph/0005004
Marzke, R. O., Geller, M. J., Huchra, J. P. & Corvin, H. G. 1994, AJ, 108, 437
Olive, K. A., Steigman, G. & Walker, T. P. 2000, astro-ph/9905320
Oukbir, J. & Blanchard, A. 1992, A& A, 262, L21
Peacock, J. A. & Dodds, S. J. 1994, MNRAS, 267, 1020
Peebles, P. J. E. 1971, in Physical Cosmology, (Princeton University Press, Princeton)
Peebles, P. J. E. 1999, in Formation of Structure in the Universe, eds Dekel, A. & Ostriker, J. P. (Cambridge University Press, Cambridge), p. 435
Perlmutter, S. et al. 1999, ApJ, 517, 565
Reid, I. N. 1997, AJ, 114, 161
Riess, A. G. et al. 1998, AJ, 116, 1009
Saha, A. et al. 1999, 522, 802
Sugiyama, N. 1995, ApJS, 100, 281
Tegmark, M. & Zaldarriaga, M. 2000, astro-ph/0004393
Tytler, D., O'Meara, J. M., Suzuki, N. & Lubin, D. 2000, astro-ph/0001318
Tytler, D. et al. 1999, AJ, 117, 63
White, D. A. & Fabian, A. C. 1995, MNRAS, 273, 72